Taylor & Francis
Taylor & Francis Group

Electromagnetic Biology and Medicine

ISSN: 1536-8378 (Print) 1536-8386 (Online) Journal homepage: www.tandfonline.com/journals/iebm20

Quantitative proteomics reveals effects of environmental radiofrequency electromagnetic fields on embryonic neural stem cells

Guangzhou An, Yuntao Jing, Tao Zhao, Wei Zhang, Ling Guo, Juan Guo, Xia Miao, Junling Xing, Jing Li, Junye Liu & Guirong Ding

To cite this article: Guangzhou An, Yuntao Jing, Tao Zhao, Wei Zhang, Ling Guo, Juan Guo, Xia Miao, Junling Xing, Jing Li, Junye Liu & Guirong Ding (2023) Quantitative proteomics reveals effects of environmental radiofrequency electromagnetic fields on embryonic neural stem cells, Electromagnetic Biology and Medicine, 42:2, 41-50, DOI: 10.1080/15368378.2023.2243980

To link to this article: https://doi.org/10.1080/15368378.2023.2243980

View supplementary material

Published online: 07 Aug 2023.

Submit your article to this journal

Article views: 172

View related articles

View Crossmark data

Citing articles: 1 View citing articles

Full Terms & Conditions of access and use can be found at
https://www.tandfonline.com/action/journalInformation?journalCode=iebm20

ELECTROMAGNETIC BIOLOGY AND MEDICINE
2023, VOL. 42, NO. 2, 41–50
https://doi.org/10.1080/15368378.2023.2243980

Taylor & Francis
Taylor & Francis Group

Check for updates

Quantitative proteomics reveals effects of environmental radiofrequency electromagnetic fields on embryonic neural stem cells

Guangzhou An[a], Yuntao Jing[a], Tao Zhao[b], Wei Zhang[a], Ling Guo[a], Juan Guo[a], Xia Miao[a], Junling Xing[a], Jing Li[a], Junye Liu[a], and Guirong Ding[a]

[a]Department of Radiation Protection Medicine, Ministry of Education Key Laboratory of Hazard Assessment and Control in Special Operational Environment, Faculty of Preventive Medicine, Air Force Medical University, Xi'an City, Shannxi Province, China; [b]Medical College, Xijing University, Xi an City, Shannxi Province, China

ABSTRACT

The effects of environmental radiofrequency electromagnetic fields (RF-EMF) on embryonic neural stem cells have not been determined, particularly at the proteomic level. This study aims to elucidate the effects of environmental levels of RF-EMF radiation on embryonic neural stem cells. Neuroectodermal stem cells (NE-4C cells) were randomly divided into a sham group and an RF group, which were sham-exposed and continuously exposed to a 1950 MHz RF-EMF at 2 W/kg for 48 h. After exposure, cell proliferation was determined by a Cell Counting Kit-8 (CCK8) assay, the cell cycle distribution and apoptosis were measured by flow cytometry, protein abundance was detected by liquid chromatography-tandem mass spectrometry (LC–MS/MS), and mRNA expression was evaluated by quantitative reverse transcription polymerase chain reaction (qRT-PCR). We did not detect differences in cell proliferation, cell cycle distribution, and apoptosis between the two groups. However, we detected differences in the abundance of 23 proteins between the two groups, and some of these differences were consistent with alterations in transcript levels determined by qRT-PCR ($P < 0.05$). A bioinformatics analysis indicated that the differentially regulated proteins were mainly enriched in 'localization' in the cellular process category; however, no significant pathway alterations in NE-4C cells were detected. We conclude that under the experimental conditions, low-level RF-EMF exposure was not neurotoxic but could induce minor changes in the abundance of some proteins involved in neurodevelopment or brain function.

ARTICLE HISTORY
Received 6 September 2022
Accepted 22 July 2023

KEYWORDS
embryo development; NE-4C cells; neurodevelopment; proteomics; radiofrequency electromagnetic fields

Introduction

The bioeffects of environmental radiofrequency electromagnetic field (RF-EMF), mainly originating from modern communication devices such as cellular phones, have become a major public health issue, attracting the mounting attention of researchers. The intensity and radius of environmental RF-EMF radiation are still growing due to the development of communication techniques and the increased use of electromagnetic products. The implementation of specific policies restricting the RF-EMF intensity aimed at reducing public exposure has led to a low-level RF-EMF with a specific absorption rate (SAR) value of <2 W/kg for individual localized exposure (IEEE 2010). However, the safety of environmental RF-EMF is still unclear (Jaffar et al. 2019; Pacchierotti et al. 2021). RF-EMF covers frequencies from 3 kHz to 300 GHz (IEEE 2010). Within this range, 1950 MHz is widely applied in universal mobile telecommunications system and has become an important component of environmental RF-EMF. Low-level 1950 MHz RF-EMF exposure could inhibit the cell proliferation and secretion of Leydig cells, increase the micronucleus frequency of fibroblasts, and enhance X-ray-induced apoptosis in spermatocyte-derived cells. However, its influence on stem cells, which are highly sensitive to electromagnetic radiation, has not been explored (Lin et al. 2017; Markovà et al. 2010; Sannino et al. 2017; Zhang et al. 2017).

Embryonic neural stem cells have the potential to differentiate into neurons or glial cells and play a vital role in embryonic neurodevelopment. Of note, every year, approximately 3.2 million children worldwide are born with a congenital anomaly. Congenital anomalies are the leading cause of perinatal mortality in Europe and approximately 5% of cases are ascribed to environmental exposure according to the World Health Organization (Baldacci et al. 2018). While the definite

CONTACT Jing Li jingli@fmmu.edu.cn; Junye Liu junyeliu@fmmu.edu.cn; Guirong Ding dingzhao@fmmu.edu.cn Department of Radiation Protection Medicine, Ministry of Education Key Laboratory of Hazard Assessment and Control in Special Operational Environment, Faculty of Preventive Medicine, Air Force Medical University, Xi'an City, Shannxi Province 710032, China

Supplemental data for this article can be accessed online at https://doi.org/10.1080/15368378.2023.2243980

© 2023 Taylor & Francis Group, LLC

bioeffects of high-level RF-EMF exposure with a SAR value of >4 W/kg have been characterized, the bioeffects of low-level environmental RF-EMF exposure and its non-thermal effects on embryonic neural stem cells are still unclear. Some studies have indicated that environmental RF-EMF exposure could affect embryonic neural stem cells and resulting embryo development. Epidemiological investigations have revealed that prenatal exposure to RF-EMF from mobile phones could increase the frequencies of migraines or headaches in children over those of children with no prenatal RF-EMF exposure (Sudan 2012). *In vivo* studies have demonstrated that RF-EMF exposure from cellular phones may impact fetal neurotransmitters and oxidative stress, and prenatal RF-EMF exposure could change the number or morphology of fetal brain cells (Jing et al. 2012; Sharma et al. 2017). *In vitro* studies have found that RF-EMF exposure could affect transcript levels of apoptosis-related genes in embryonic stem cell-derived neural progenitor cells (Nikolova et al. 2005). However, some studies have not detected the effects of low-level RF-EMF exposure on embryonic neural stem cells and embryonic development (Bornhausen and Scheingraber 2000; Jensh 1997; Lary et al. 1983).

Embryonic stem cells could provide important insight into genetic and epigenetic events at the early stage of embryonic development (Okae et al. 2018; Rossant and Tam 2018). As a kind of embryonic neural stem cells, the NE-4C cell line is the appropriate model to study neurodevelopment in the embryo and to evaluate neurotoxicity of environmental factors (Milatovic et al. 2011; Tamm et al. 2008). Differentially expressed proteins across time and space determine the direction of cellular differentiation and the ultimate fate of cells. However, the effects of environmental RF-EMF exposure on genome-wide protein expression in embryonic neural stem cells have not been elucidated to date. Therefore, NE-4C cells were selected in this study to evaluate the effects of environmental level RF-EMF on embryonic neural stem cells from a proteomics perspective.

Materials and methods

Cell culture

The NE-4C cell line derived from neuroectodermal tissue of a mouse embryo was obtained from the Stem Cell Bank of the Chinese Academy of Sciences (Shanghai, China) and cultured in Minimum Essential Medium (MEM) supplemented with 10% fetal bovine serum, 2 mM glutamine and 100× penicillin–streptomycin (Invitrogen; Thermo Fisher Scientific Corporation, Carlsbad, CA, USA). NE-4C cells were cultured on 0.01% poly-L-lysine (Sigma – Aldrich, Saint Louis, Missouri, USA) precoated culture dishes (diameter 35 mm; NUNC, Thermo Fisher Scientific) and incubated at 37°C in a humidified air containing 5% CO_2. After reaching approximately 85% confluence, cells were subcultured at a 1:6 ratio. NE-4C cells were seeded onto culture dishes precoated with poly-L-lysine and incubated for 24 h at 37°C before RF-EMF exposure.

RF-EMF exposure setup

The RF-EMF setup (sXc-RF, IT'IS foundation, Zurich, Switzerland) was composed of two rectangular waveguide cavities, one incubator, one RF-EMF generator, one arbitrary function generator and one narrow band amplifier (Figure 1). RF-EMF in waveguides was activated by couplers and removable shortcuts. There was one petri dish holder in each waveguide, and each petri dish holder could hold six NUNC petri dishes. One waveguide was set for RF-EMF exposure, while the other one was set for the sham control without RF-EMF exposure. The RF-EMF generator can generate an RF-EMF signal that could be modulated by the arbitrary function generator. The temperature in the waveguide was monitored with Pt100 probes fixed on the top of each fan. The RF-EMF exposure system was connected to a personal computer able to set and monitor the exposure parameters using sXcRF Experimental Control Software Version 3.2b2. The environment in the waveguides of the incubator was maintained at 37°C and 5% CO_2. The temperature difference between the two waveguides did not exceed 0.1°C during RF-EMF exposure.

RF-EMF exposure

NE-4C cells at the exponential growth stage were seeded onto 35 mm NUNC dishes at 1×10^5 cells per dish. At 24 h after seeding, the cell culture medium was replaced with 2.5 mL fresh medium, and cells in dishes were placed in the two waveguides. One waveguide was set to the RF-EMF exposure chamber, and cells in three dishes were continuously exposed to 1950 MHz RF-EMF for 48 h at an average SAR of 2 W/kg. The other waveguide was used for a sham treatment, and cells in three dishes were kept under the same experimental conditions without RF-EMF exposure. The RF-EMF exposure parameters were verified by a forward power sensor and meter before the experiment and were monitored by a backward power sensor and meter during the whole exposure experiment. The temperature was maintained at 37°C during the RF-EMF exposure in

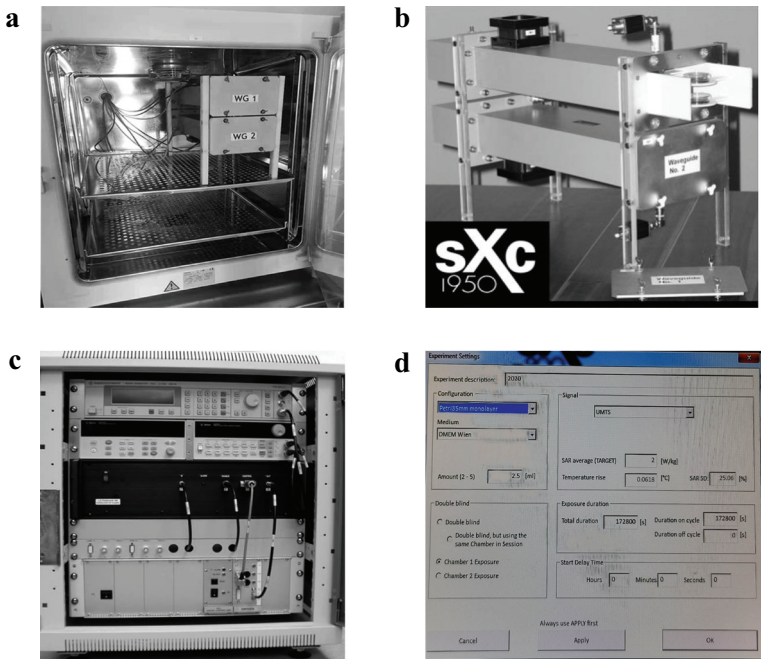

Figure 1. 1950 MHz RF-EMF Setup. (a) the cell incubator with waveguide cavities. (b) Waveguide cavities containing the waveguide chamber, petri dish holder, field detector, ventilator and temperature sensor. (c) the rack with the RF-EMF signal generator, RF-EMF power amplifier, function generator, data acquisition unit and digital control unit. (d) the PC software for setting and monitoring the RF-EMF exposure parameters.

the waveguides. After RF-EMF exposure, cellular morphology was observed under an inverted microscope, cell proliferation was determined by the CCK8 assay, and cell cycle distribution and apoptosis were measured by flow cytometry.

CCK8 assay

NE-4C cells were digested by 0.05% trypsin solution (Invitrogen) and centrifuged at $150 \times g$ for 5 min. Supernatants were discarded, and cell pellets were resuspended with culture medium. The cell concentration was adjusted to 5×10^3 cells/mL, and 200 µL of the cell suspension was added to each well of 96-well microplates (Corning, NYC, NY, USA). At intervals of 24 h, 10 µL of CCK-8 reagent (Beyotime, Shanghai, China) was added to each well and cultured for 2 h. Absorbance was detected at 450 nm using a microplate reader (Thermo Fisher Scientific). Cell proliferation was quantified by the optical density (OD).

Flow cytometry assay

To detect the cell cycle distribution, NE-4C cells were harvested and washed twice with cold phosphate-buffered saline (PBS). Then, cells were fixed by pre-chilled 70% ethanol for 30 min at 4°C. After centrifugation, cells were stained with 50 µg/ml propidium iodide (PI, Sigma-Aldrich, St. Louis, MO, USA) mixed with PBS for 30 min at 37°C, followed by the detection of the cell cycle distribution using the FACSCalibur Flow Cytometer (BD Biosciences, San Jose, CA, USA).

Harvested NE-4C cells along with their culture medium were centrifuged at 1000 rpm for 5 min for analysis of apoptosis. Pellets were resuspended in a binding buffer and stained with 5 µL Annexin V-FITC plus 5 µL PI (Sigma-Aldrich) at 4°C for 30 min in the dark. Stained cells were washed by binding buffer three times to remove excess dyes and then resuspended in 500 µL binding buffer. The percentage of apoptosis was analyzed using the FACSCalibur Flow Cytometer (BD Biosciences) within 1 h.

Total protein extraction and peptide preparation

Total protein extraction, peptide preparation, and quantitative proteomic analysis were performed according to the previously reported methodology, with some modifications (Guerrero-Castillo et al. 2021; Sathe et al. 2021). Upon the end of RF-EMF exposure, cells in sham group and RF group were harvested immediately with a cell scraper, followed by centrifugation at $1500 \times g$ for 10 min and washing with PBS twice. Cells were lysed with a lysis buffer containing 7 M urea (Sigma-Aldrich), 0.2% sodium dodecyl sulfate (SDS, Sigma-Aldrich) and 1× protease inhibitor cocktail (Sigma-

Aldrich). Samples were then treated by ultrasonication on ice (2 s-on and 7 s-off) for 1 min and kept on ice for 2 h. The lysate was centrifuged at 1200 × *g* for 20 min at 4°C and the middle layer was transferred to a clean tube, followed by mixing it with six volumes of acetone (Sigma-Aldrich). The mixture was maintained at −20°C overnight. The next day, the mixture was centrifuged and the collected precipitate was washed twice with a precooled mixed solution (ethanol: acetone: acetic acid = 50:50:0.1), followed by centrifugation at 12,000 × *g* for 15 min at 4°C. Pellets were dissolved again by the mixed solution containing 6 M guanidine hydrochloride (Sigma-Aldrich) and 300 mM triethylammonium bicarbonate (TEAB, Sigma-Aldrich). Samples were kept at 4°C and protein concentration was determined with a BCA Kit (Nanjing Jiancheng Bioengineering Institute, Nanjing, China) according to the manufacturer's instructions. Then, 150 μg of each sample was diluted with TEAB to 100 μL.

Filter aided proteome preparation enzymolysis was carried out as follows: Samples were transferred to the 10 K ultrafiltration tube (Millipore, MA, USA), centrifuged at 12,000 × *g* and the flowthrough was discarded. Ultrafiltration tubes were washed four times with TEAB (dissolution buffer). Trypsin solution prepared by the dissolution buffer was added to the ultrafiltration tubes and maintained at 37°C overnight for enzymolysis. The peptides were collected by vacuum centrifugation and were redissolved with a dissolution buffer to 200 μL. Peptide labeling was performed using the tandem mass tag (TMT) 6plex™ Isobaric Label Reagent Set (Thermo Fisher Scientific) following manufacturer's instructions.

For desalination, peptides were dissolved with 0.1% trifluoroacetic acid (TFA, Sigma-Aldrich). Monospin desalination columns (Shimadzu Corporation, Tokyo, Japan) were activated with 100% acetonitrile (Sigma-Aldrich) and then balanced with 0.1% TFA. The dissolved samples were transferred to desalination columns and centrifuged. Desalination columns were washed with 0.1% TFA. Then, 50% acetonitrile was added to desalination columns and peptides were collected into a new tube after centrifugation. The eluates were centrifuged and dried to remove acetonitrile.

Peptides were redissolved in 0.1% TFA solution and fractionated by applying a Pierce High pH Reversed-Phase Peptide Fractionation Kit (Cat. No. 84868, Thermo Fisher Scientific) following the manufacturer's instructions. The absorbance of eluates was measured at 214 nm UV. They were collected at one tube per minute and finally 10 total fractions were gained. All fractions were then vacuum-centrifuged and maintained in dry condition.

LC – MS/MS analysis

Each dried sample of sham group and RF group was reconstituted with 0.1% (v/v) formic acid (FA, Sigma-Aldrich) in water and 2 μg of each sample was added to the EASY-nLC 1200 Liquid Chromatography System (Thermo Fisher Scientific). The peptides were separated using an in-house analytical column (C18 reversed-phase column, 2 μm, 75 μm × 250 mm; Thermo Fisher Scientific) by linear gradient elution from 0% to 50% B (A = 0.1% FA; B = 80% acetonitrile, 0.1% FA) at a flow velocity of 200 nL/min over 120 min. The Orbitrap Fusion Lumos Mass Spectrometer (Thermo Fisher Scientific) was operated in the data-dependent mode with a cycle time of 3 s and automated precursor peak selection. Spectra were gained in the positive-ionization mode at an electrospray voltage of 2400 V. The full scan resolution was 6×10^4 (FWHM), the mass-to-charge ratio (m/z) was set to 350–1600, and the collision energy was set to 30% in the higher-energy collision dissociation (HCD) fragmentation model.

Differentially regulated proteins screening

Raw data were searched using Proteome Discoverer 2.4 (Thermo Fisher Scientific) with the SEQUEST search algorithm against the Swissprot database. Trypsin was selected as the protease and a maximum of two missed cleavages were allowed. Peptide mass was set to 10 ppm, and MS/MS tolerance was set to ±0.02 Da. Fixed modifications were selected for Carbamidomethyl (C), TMT 6plex (N-term), TMT 6plex (K), Acetyl (N-Term) Met-loss (M) and Met-loss + Acetyl (M). Met oxidation was used as a variable modification. The false discovery rate was set to 1% at the peptide and protein levels.

To screen differentially regulated proteins, the Student's t-test was used to evaluate differences between the RF group and the sham group. Differentially regulated proteins were determined by the following thresholds: fold change ≥1.1 or ≤0.909 and $P < 0.05$. Differentially regulated proteins were visualized as a heatmap and volcano plot generated using RStudio 3.6.0.

Bioinformatic analysis

Gene Ontology (GO), Kyoto Encyclopedia of Genes and Genomes (KEGG), and protein–protein interaction (PPI) network analyses of differentially expressed genes (DEGs) were performed. GO and KEGG analyses were performed using the online platform DAVID (https://david.ncifcrf.gov/). GO terms were identified in three general categories: biological processes (BP),

Table 1. Specific primer sequence.

Gene Symbol (Mus)	Primer sequence
Bbs1	CCTCATGGACCAACACGAGC
	GTTCCAAACGTCCTGTTCCAA
Slc38a3	GGAGGGGCTTCTACCAGTG
	AAAGGATGATGCCCGTATTGG
Myo9a	AGGAAGACGACGCTTTGAGG
	CTGGCAGGAATTGGACAGTAAA
Hexb	GAGTGCGAGTCCTTCCCTAGT
	CTAAACCTCGTAACGCTCCCC
Tmod2	GGCCTGTGAGGAATGTCGTG
	TCCTTCAGGGTTGGAATTGGA
Slc3a2	TGATGAATGCACCCTTGTACTTG
	GCTCCCCAGTGAAAGTGGA
Vps18	ATGGCCGAGGCTTTGTCATT
	CCCTGGGCTTCAGTATCTTCC
Zfp106	GCCACATCGTGTATGGCTCAA
	TCAGGTTCTCAAGTTCCCTGT
Gapdh	GGTGAAGGTCGGTGTGAACG
	CTCGCTCCTGGAAGATGGTG

cellular components (CC), and molecular functions (MF). GO and KEGG analysis results were visualized using the R packages 'GOplot' and 'ggplot2', respectively. $P < 0.05$ was defined as statistically significant for both analyses. A PPI analysis of the DEGs was carried out using the STRING database, and the medium confidence was set to 0.400 (version 11.5, https://string-db.org/cgi/input.pl). Hub genes were defined by rank values of connectivity.

qRT-PCR analysis

Total RNA was extracted from NE-4C cells using a GeneJET RNA Purification Kit (Thermo Fisher Scientific) following the manufacturer's instructions. cDNA synthesis was conducted using the PrimeScript™ Reverse Transcription Master Mix Kit （Takara Bio Inc, Shiga, Japan）according to the manufacturer's instructions. TB Green Premix Ex TaqTM II (Takara Bio Inc) was used for real-time PCR with the CFX384 Real-Time system (Bio-Rad Laboratories, Hercules, CA, USA) under the following conditions: 95°C for 30 s and 40 cycles of 95°C for 5 s and 60°C for 30 s. Real-time RT-PCR for target gene quantification was performed in quadruplicate. Specific primers are displayed in Table 1. The results were based on $2^{-\Delta\Delta ct}$ values and mouse *Gapdh* served as an internal reference gene.

Data management and statistical analysis

The raw MS spectral data and search data have been deposited in the ProteomeXchange Consortium (http://proteomecentral.proteomexchange.org) via the iProX partner repository with the dataset identifier **PXD031285**. All experiments were conducted at least in triplicate, and data analysis was performed using SPSS 17.0. Statistical significance was assessed using Student's t-tests. $P < 0.05$ was defined as statistically significant.

Results

NE-4C cell toxicity induced by low-level RF-EMF exposure

The morphology of cells in the two groups was the same in size and no detrimental signs such as vacuoles were found in cells under the microscope. The cell alignment was regular and cell status was normal in both groups (Figure 2A, B). There was no significant difference in cell proliferation between the sham-exposed group and the RF-EMF exposed group determined by a CCK8 assay ($P > 0.05$) (Figure 2C). A flow cytometry assay showed that 48 h low-level RF-EMF exposure did not affect the cell cycle distribution (Figure 2D) or induce apoptosis in NE-4C cells ($P > 0.05$) (Figure 2E).

Identification of differentially regulated proteins and bioinformatic analysis of DEGs

We identified and quantified 40,512 peptides and 5,369 proteins by TMT-based proteomics, of which 12 proteins were up-regulated and 11 proteins were down-regulated by RF-EMF exposure ($P < 0.05$). Differentially regulated proteins are visualized in a heatmap (Figure 3A) and volcano plot (Figure 3B). The fold change values of the upregulated proteins ranged from 1.11 to 1.19, and those of the downregulated proteins ranged from 0.78 to 0.91. All differentially regulated proteins and related information are provided in Supplemental Table 1. The GO analysis results revealed that the DEGs were mainly enriched in 'localization' in the BP category. In the CC category, DEGs were mainly enriched for the term 'cytoplasm'. In the MF category, the DEGs were mainly enriched in the term 'protein binding'. The enriched GO terms are shown in Figure 3C. The KEGG analysis showed that the DEGs were involved in multiple pathways, including 'proximal tubule bicarbonate reclamation' and 'mismatch repair'. However, the differences in these pathways between groups were not significant (Figure 3D). In PPI network analysis of DEGs, we found no hub genes. There was no interaction between the DEGs, except for an interaction between Slc3a2 and Slc38a3 (Figure 3E).

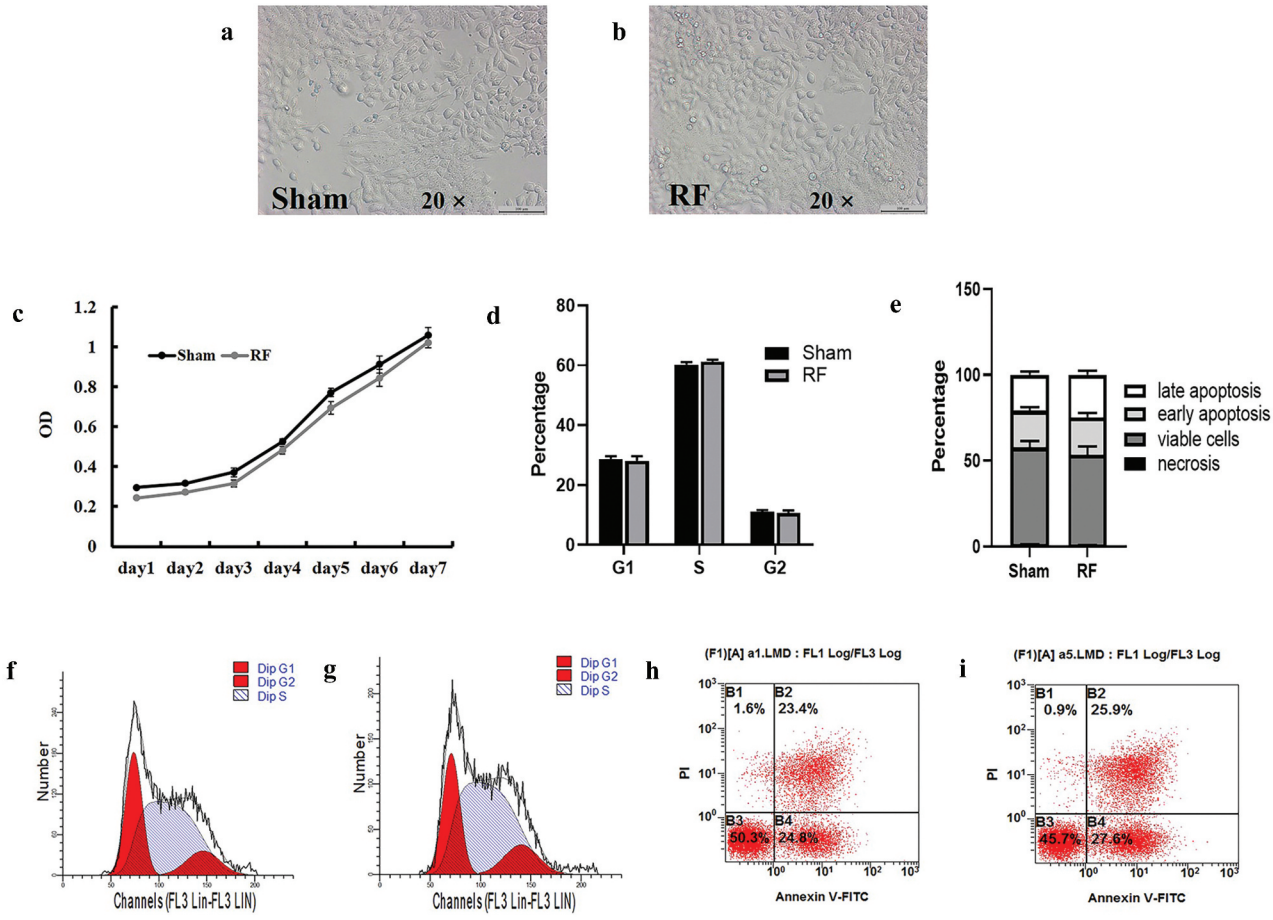

Figure 2. Low-level RF-EMF exposure did not cause neurotoxic effects. (a) the morphology of NE-4C cells in the sham group (200 folds magnification). (b) the morphology of NE-4C cells in the RF group (200 folds magnification). (c) Cell proliferation was assessed by CCK8 assay. (d) the distribution of cell cycle was measured by flow cytometry. (e) the apoptosis rate was measured by flow cytometry. (f) the representative flow cytometry plot of cell cycle in the sham group. (g) the representative flow cytometry plot of cell cycle in the RF group. (h) the representative flow cytometry plot of apoptosis in the sham group. (i) the representative flow cytometry plot of apoptosis in the RF group. Data are presented as mean ± SEM of three independent experiments.

qRT-PCR results of DEGs directly related to neurodevelopment or brain function

qRT-PCR results confirmed that the expression levels of *Bbs1* and *Slc38a3* that directly related to neurodevelopment and *Vps18*, which was directly related to brain function, were significantly upregulated at the transcription level in the RF group compared with the sham group ($P < 0.05$) (Figure 4A, B, G). However, the expression of the other five genes (*Myo9a*, *Hexb*, *Tmod2*, *Slc3a2*, *Zfp106*) directly related to neurodevelopment or brain function did not differ between the sham group and the RF group ($P > 0.05$) (Figure 4C, D, E, F, H).

Discussion

Embryo development is a finely regulated and highly dynamic process characterized by the persistent proliferation and differentiation of embryo stem cells, which are highly sensitive to environmental stressors. However, the relationship between environmental RF-EMF and embryo stem cells is not well elucidated, and little is known about the related molecular mechanisms. In our study, we found that short-term low-level RF-EMF exposure did not affect the morphology, proliferation, cell cycle distribution, and apoptosis of NE-4C cells, indicating a lack of neurotoxicity or direct damage to embryonic stem cells or embryos. Several studies of stem cells have reported consistent results. For example, 900 MHz RF-EMF exposure at a SAR of 2.287 W/Kg did not influence cell viability and apoptosis of neural stem cells (Eghlidospour et al. 2017). In another study, low-level RF-EMF exposure (900, 1950 or 2535 MHz) did not affect the apoptosis or the cell cycle distribution in human hematopoietic stem cells (Gläser et al. 2016). However, other studies have shown that low-level RF-

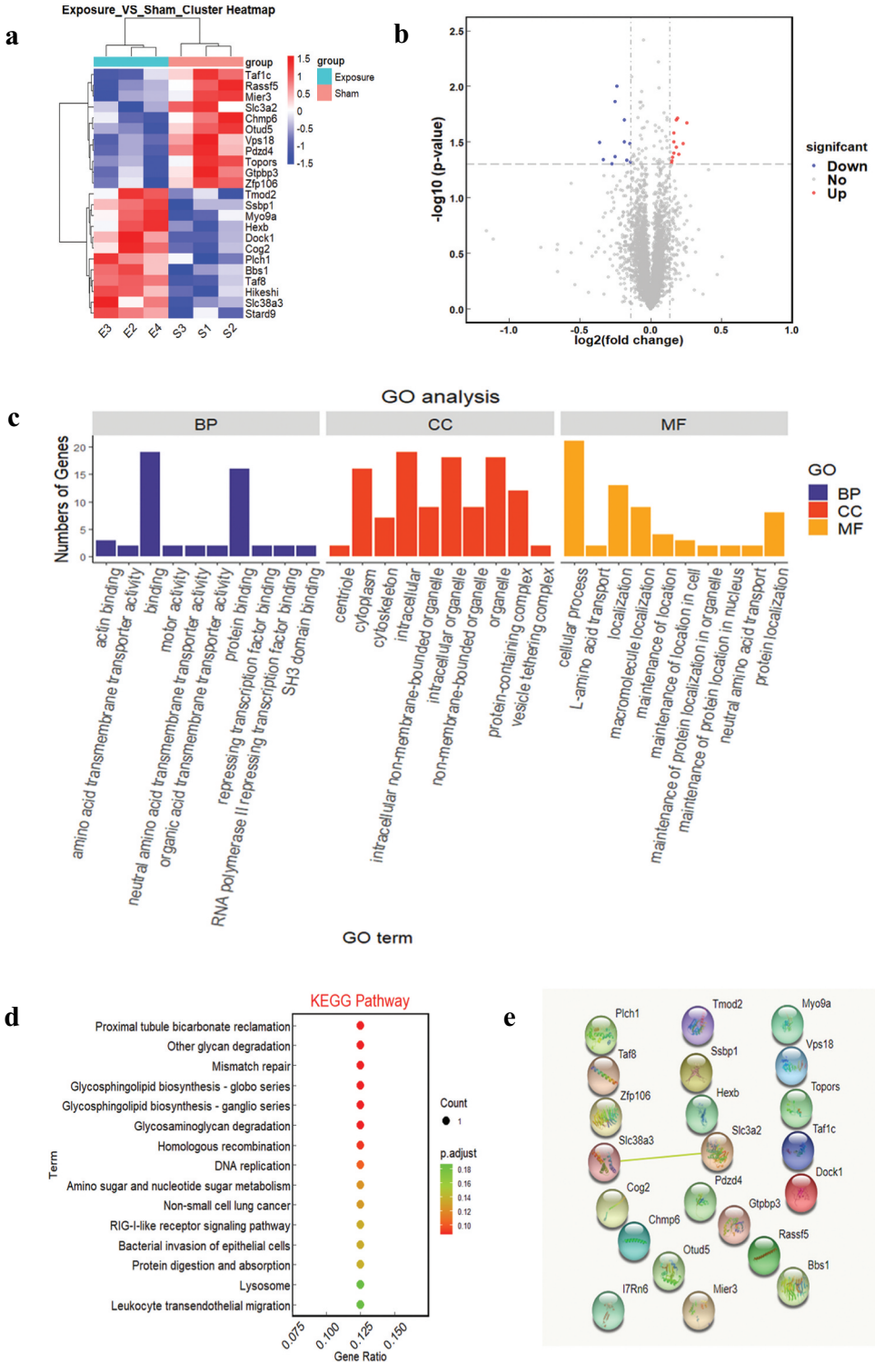

Figure 3. Low-level RF-EMF exposure could potentially change protein levels and corresponding DEGs were analyzed using bioinformatic methods. (a) Rows represent proteins and columns represent samples in the heatmap. (b) Red spots represent significantly upregulated proteins and the blue spots represent significantly downregulated proteins in the volcano plot. (c) Functional enrichment analysis of DEGs. (d) Pathway enrichment analysis of DEGs. (e) PPI network of DEGs.

EMF exposure (i.e., 900 MHz) could significantly inhibit the proliferation of Michigan Cancer Foundation (MCF-7) cells and human adipose-derived stem cells, and similar results have been found in other cell lines, such as V79 cells (Čermak et al. 2020; Shahbazi-Gahrouei et al. 2018). The inconsistency among studies can possibly be due to the difference in cell lines and RF-EMF exposure parameters.

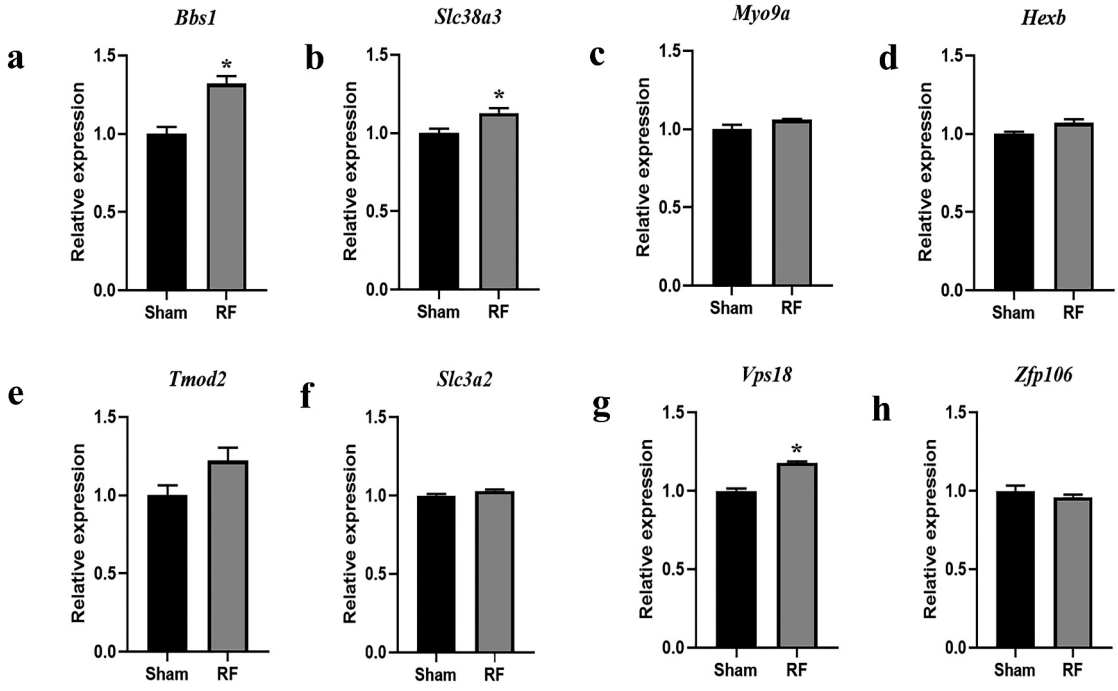

Figure 4. Qrt-PCR results confirmed that low-level RF-EMF exposure could change the expression of several genes directly related to neurodevelopment or brain function. (A-H) the relative expression of *Bbs1*, *Slc38a3*, *Myo9a*, *Hexb*, *Tmod2*, *Slc3a2*, *Vps18* and *Zfp106* in sequence. Data are presented as mean ± SEM of four independent experiments. * vs. sham group, $P < 0.05$.

To further explore the effects of low-level RF-EMF exposure on embryonic neural stem cells at the molecular level, we analyzed the proteomic changes in NE-4C cells by applying the mass spectrometric technique that tended to be applied in high-level RF-EMF exposure experiments other than low-level RF-EMF exposure experiments, and identified 23 differentially regulated proteins, with small changes in protein abundance (Vanderstraeten and Verschaeve 2008). Proteomic analyses of embryo stem cells after low-level RF-EMF exposure are largely lacking, except for one study revealing that <1% of the quantitated proteome in mouse embryonic stem cells (IB10) was altered in response to 2.1 GHz RF-EMF exposure with fold change values of <1.5. Combined with other related high throughput analyses, we could conclude that cellular proteomics varies depending on RF-EMF parameters (Chauhan et al. 2007; Gurisik et al. 2006; Luo et al. 2013).

The proteomic analysis in this study indicated that low-level RF-EMF exposure was not absolutely safe; thus, the bioinformatic analysis was conducted to explore the potential effects. Although GO enrichment analysis showed that the differentially regulated proteins mainly contributed to localization, pathway differences between groups were not significant, indicating that the effects of low-level RF-EMF exposure are limited and are not likely to induce phenotypic changes. Therefore, it is reasonable to speculate that short-term low-level RF-EMF exposure does not affect the differentiation or function of embryonic neural stem cells. In addition, we did not detect any hub genes in the PPI network analysis, indicating that the interactions between differentially regulated proteins were weak or negligible, possibly due to the small number of differentially regulated proteins and their dispersive subcellular location.

Among 23 differentially regulated proteins, 8 proteins are directly related with neurodevelopment or brain function, namely Bardet–Biedl syndrome 1 protein homolog, mNAT, Unconventional myosin-Ixa, Hexosaminidase subunit B, N-Tmod, 4F2hc, vacuolar protein sorting-associated protein 18 homolog and Zfp-106. The differential expression of hexosaminidase subunit B, mNAT and vacuolar protein sorting-associated protein 18 homolog was verified at transcriptional level by real-time PCR. Bardet–Biedl syndrome 1 protein homolog, encoded by the gene of *Bbs1* could influence brain morphogenesis, cerebral cortex development, dendrite development, neuron migration, and neural precursor cell proliferation (Carter et al. 2012; Davis et al. 2007; Ishizuka et al. 2011; Kulaga et al. 2004). mNAT, encoded by *Slc38a3*, may contribute to synaptic transmission, thereby affecting brain development. Vacuolar protein sorting-associated protein 18 homolog, encoded by the gene of *Vps18*, plays a role in vesicle-mediated protein trafficking to lysosomal compartments and the regulation of synaptic vesicle

exocytosis. However, minor changes in the levels of these three proteins are not expected to affect the differentiation or function of NE-4C cells, according to the bioinformatic analysis. We cannot exclude the potential influence of low-level RF-EMF exposure on NE-4C cells by unknown mechanisms involving additional proteins or pathways. Moreover, further studies are needed to determine whether long-term or more intense RF-EMF exposure could increase the changes in protein abundance and thereby affect phenotypes of NE-4C cells.

Conclusions

Short-term, low-level RF-EMF exposure was not neurotoxic. Although no pathways were perturbed, minor changes in the abundance of some intracellular proteins involved in neurodevelopment or brain function in NE-4C cells induced by low-level RF-EMF should be a focus of further studies. This study provides novel insights into the effects of low-level RF-EMF exposure on embryonic neural stem cells and has implications for public health.

Disclosure statement

No potential conflict of interest was reported by the author(s).

Funding

This work was supported by the [National Natural Science Foundation of China] under grant [NO.31900888].

ORCID

Guirong Ding http://orcid.org/0000-0001-5750-6000

References

Baldacci, S., F. Gorini, M. Santoro, A. Pierini, F. Minichilli, and F. Bianchi. 2018. Environmental and individual exposure and the risk of congenital anomalies: A review of recent epidemiological evidence. *Epidemiol. Prev.* 42 :1–34. doi:10.19191/EP18.3-4.S1.P001.057.

Bornhausen, M., and H. Scheingraber. 2000. Prenatal exposure to 900 MHz, cell-phone electromagnetic fields had no effect on operant-behavior performances of adult rats. *Bioelectromagnetics* 21 :566–74. doi:10.1002/1521-186X(200012)21:8<566:AID-BEM2>3.0.CO;2-G.

Carter, C. S., T. W. Vogel, Q. Zhang, S. Seo, R. E. Swiderski, T. O. Moninger, M. D. Cassell, D. R. Thedens, K. M. Keppler-Noreuil, P. Nopoulos, et al. 2012. Abnormal development of NG2+PDGFR-alpha+ neural progenitor cells leads to neonatal hydrocephalus in a ciliopathy mouse model. *Nat. Med.* 18 :1797–804. doi:10.1038/nm.2996.

Čermak, A. M. M., K. Ilić, and I. Pavičić. 2020. Microtubular structure impairment after GSM-modulated RF radiation exposure. *Arh. Hig. Rada Toksikol.* 71 :205–10. doi:10.2478/aiht-2020-71-3267.

Chauhan, V., S. S. Qutob, S. Lui, A. Mariampillai, P. V. Bellier, C. L. Yauk, G. R. Douglas, A. Williams, and J. P. McNamee. 2007. Analysis of gene expression in two human-derived cell lines exposed in vitro to a 1.9 GHz pulse-modulated radiofrequency field. *Proteomics* 7 :3896–905. doi:10.1002/pmic.200700215.

Davis, R. E., R. E. Swiderski, K. Rahmouni, D. Y. Nishimura, R. F. Mullins, K. Agassandian, A. R. Philp, C. C. Searby, M. P. Andrews, S. Thompson, et al. 2007. A knockin mouse model of the bardet–biedl syndrome 1 M390R mutation has cilia defects, ventriculomegaly, retinopathy, and obesity. *Proc. Natl. Acad. Sci. U.S.A.* 104 :19422–27. doi:10.1073/pnas.0708571104.

Eghlidospour, M., A. Ghanbari, S. M. J. Mortazavi, and H. Azari. 2017. Effects of radiofrequency exposure emitted from a GSM mobile phone on proliferation, differentiation, and apoptosis of neural stem cells. *Anat Cell Biol.* 50 :115–23. doi:10.5115/acb.2017.50.2.115.

Gläser, K., M. Rohland, T. Kleine-Ostmann, T. Schrader, H. Stopper, and H. Hintzsche. 2016. Effect of radiofrequency radiation on human hematopoietic stem cells. *Radiat. Res.* 186 :455–65. doi:10.1667/rr14405.1.

Guerrero-Castillo, S., C. Krisp, K. Küchler, S. Arnold, H. Schlüter, and S. W. Gersting. 2021. Multiplexed complexome profiling using tandem mass tags. *Biochim. Biophys. Acta Bioenerg.* 1862 :148448. doi:10.1016/j.bbabio.2021.148448.

Gurisik, E., K. Warton, D. K. Martin, and S. M. Valenzuela. 2006. An in vitro study of the effects of exposure to a GSM signal in two human cell lines: Monocytic U937 and neuroblastoma SK-N-SH. *Cell Biol. Int.* 30 :793–99. doi:10.1016/j.cellbi.2006.06.001.

IEEE. 2010. *IEEE standard for safety levels with respect to human exposure to radio frequency electromagnetic fields, 3 kHz to 300 GHz amendment 1: Specifies ceiling limits for induced and contact current, clarifies distinctions between localized exposure and spatial peak power density*. 1st ed. USA. doi:10.1109/IEEESTD.2010.5433227.

Ishizuka, K., A. Kamiya, E. C. Oh, H. Kanki, S. Seshadri, J. F. Robinson, H. Murdoch, A. J. Dunlop, K. Kubo, K. Furukori, et al. 2011. DISC1-dependent switch from progenitor proliferation to migration in the developing cortex. *Nature* 473 :92–96. doi:10.1038/nature09859.

Jaffar, F. H. F., K. Osman, N. H. Ismail, K. Y. Chin, and S. F. Ibrahim. 2019. Adverse effects of wi-fi radiation on male reproductive system: A systematic review. *Tohoku J. Exp. Med.* 248 :169–79. doi:10.1620/tjem.248.169.

Jensh, R. P. 1997. Behavioral teratologic studies using microwave radiation: Is there an increased risk from exposure to cellular phones and microwave ovens? *Reprod. Toxicol.* 11 :601–11. doi:10.1016/S0890-6238(97)89179-4.

Jing, J., Z. Yuhua, Y. Xiao-Qian, J. Rongping, G. Dong-Mei, and C. Xi. 2012. The influence of microwave radiation from cellular phone on fetal rat brain. *Electromagn Biol. Med.* 31 :57–66. doi:10.3109/15368378.2011.624652.

Kulaga, H. M., C. C. Leitch, E. R. Eichers, J. L. Badano, A. Lesemann, B. E. Hoskins, J. R. Lupski, P. L. Beales, R. R. Reed, and N. Katsanis. 2004. Loss of BBS proteins

causes anosmia in humans and defects in olfactory cilia structure and function in the mouse. *Nat. Genet.* 36 :994–98. doi:10.1038/ng1418.

Lary, J. M., D. L. Conover, and P. H. Johnson. 1983. Absence of embryotoxic effects from low-level (nonthermal) exposure of rats to 100 MHz radiofrequency radiation. *Scand. J. Work Environ. Health* 9 :120–27. doi:10.5271/sjweh.2434.

Lin, Y. Y., T. Wu, J. Y. Liu, P. Gao, K. C. Li, Q. Y. Guo, M. Yuan, H. Y. Lang, L. H. Zeng, and G. Z. Guo. 2017. 1950mhz radio frequency electromagnetic radiation inhibits testosterone secretion of mouse leydig cells. *Int. J. Environ. Res. INT. J. ENVIRON. RES.* 15 :17. doi:10.3390/ijerph15010017.

Luo, Q., Y. Jiang, M. Jin, J. Xu, and H. F. Huang. 2013. Proteomic analysis on the alteration of protein expression in the early-stage placental villous tissue of electromagnetic fields associated with cell phone exposure. *Reprod. Sci.* 20 :1055–61. doi:10.1177/1933719112473660.

Markovà, E., L. O. Malmgren, and I. Y. Belyaev. 2010. Microwaves from mobile phones inhibit 53BP1 focus formation in human stem cells more strongly than in differentiated cells: Possible mechanistic link to cancer risk. *Environ. Health Perspect.* 118 :394–99. doi:10.1289/ehp.0900781.

Milatovic, D., R. C. Gupta, Y. Yu, S. Zaja-Milatovic, and M. Aschner. 2011. Protective effects of antioxidants and anti-inflammatory agents against manganese-induced oxidative damage and neuronal injury. *Toxicol. App. l Pharmacol.* 256 :219–26. doi:10.1016/j.taap.2011.06.001.

Nikolova, T., J. Czyz, A. Rolletschek, P. Blyszczuk, J. Fuchs, G. Jovtchev, J. Schuderer, N. Kuster, and A. M. Wobus. 2005. Electromagnetic fields affect transcript levels of apoptosis-related genes in embryonic stem cell-derived neural progenitor cells. *Faseb j.* 19 :1686–88. doi:10.1096/fj.04-3549fje.

Okae, H., H. Toh, T. Sato, H. Hiura, S. Takahashi, K. Shirane, Y. Kabayama, M. Suyama, H. Sasaki, and T. Arima. 2018. Derivation of human trophoblast stem cells. *Cell Stem Cell* 22 :50–63 e6. doi:10.1016/j.stem.2017.11.004.

Pacchierotti, F., L. Ardoino, B. Benassi, C. Consales, E. Cordelli, P. Eleuteri, C. Marino, M. Sciortino, M. H. Brinkworth, G. Chen, et al. 2021. Effects of radiofrequency electromagnetic field (RF-EMF) exposure on male fertility and pregnancy and birth outcomes: Protocols for a systematic review of experimental studies in non-human mammals and in human sperm exposed in vitro. *Environ Int* 157:106806. doi:10.1016/j.envint.2021.106806.

Rossant, J., and P. P. L. Tam. 2018. Exploring early human embryo development. *Science* 360 :1075–76. doi:10.1126/science.aas9302.

Sannino, A., O. Zeni, S. Romeo, R. Massa, and M. R. Scarfi. 2017. Adverse and beneficial effects in Chinese hamster lung fibroblast cells following radiofrequency exposure. *Bioelectromagnetics* 38 :245–54. doi:10.1002/bem.22034.

Sathe, G., M. Albert, J. Darrow, A. Saito, J. Troncoso, A. Pandey, and A. Moghekar. 2021. Quantitative proteomic analysis of the frontal cortex in alzheimer's disease. *J. Neurochem.* 156 :988–1002. doi:10.1111/jnc.15116.

Shahbazi-Gahrouei, D., B. Hashemi-Beni, A. Moradi, M. Aliakbari, and S. Shahbazi-Gahrouei. 2018. Exposure to global system for mobile communication 900 MHz cellular phone radiofrequency alters growth, proliferation and morphology of Michigan cancer foundation-7 cells and mesenchymal stem cells. *Int. J. Prev. Med.* 9 :51. doi:10.4103/ijpvm.IJPVM_75_17.

Sharma, A., K. K. Kesari, V. K. Saxena, and R. Sisodia. 2017. The influence of prenatal 10 GHz microwave radiation exposure on a developing mice brain. *Gen. Physiol. Biophys.* 36 :41–51. doi:10.4149/gpb_2016026.

Sudan, M. 2012. Prenatal and Postnatal Cell Phone Exposures and Headaches in Children. *Open Pediatr. Med. J.* 6 :46–52. doi:10.2174/1874309901206010046.

Tamm, C., F. Sabri, and S. Ceccatelli. 2008. Mitochondrial-mediated apoptosis in neural stem cells exposed to manganese. *Toxicol. Sci.* 101 :310–20. doi:10.1093/toxsci/kfm267.

Vanderstraeten, J., and L. Verschaeve. 2008. Gene and protein expression following exposure to radiofrequency fields from mobile phones. *Environ. Health Perspect.* 116 :1131–35. doi:10.1289/ehp.11279.

Zhang, K. Y., H. Xu, L. Du, J. L. Xing, B. Zhang, Q. S. Bai, Y. Q. Xu, Y. C. Zhou, J. P. Zhang, Y. Zhou, et al. 2017. Enhancement of X-ray induced apoptosis by mobile phone-like radio-frequency electromagnetic fields in mouse spermatocyte-derived cells. *Int. J. Environ. Res. INT. J. ENVIRON. RES.* 14 :616. doi:10.3390/ijerph14060616.